

Laser & Optoelectronics Progress

Observation of Parity-Time Symmetry Breaking in Single-Photon Interferometer

Meng Zhe, Guo Xue, Chen Xiaoxiao, Yang Jiazhi, Li Jian, Mairikena Aili, Zhang Anning*

Center for Quantum Technology Research and Key Laboratory of Advanced Optoelectronic Quantum Architecture and Measurements (MOE), School of Physics, Beijing Institute of Technology, Beijing 100081, China

Abstract We experimentally simulate a parity-time (PT)-symmetric quantum dynamics in a non-Hermitian system using a single-photon interferometer. We measure quantum final state using quantum state tomography. We observe the quantum state evolutions ranging from regions of unbroken to broken PT-symmetry using the single-photon interferometer. We experimentally prove that the eigenvalue of energy changes from real to imaginary corresponding to the non-Hermitian system from the PT-symmetry unbroken region to the PT-symmetry broken region. To the best of our knowledge, this is the first work to intuitively show the exceptional points of PT-symmetry non-unitary quantum dynamics in a single-photon interferometer from the energy perspective.

Key words quantum optics; parity-time symmetry; single-photon interferometer; non-Hermitian system

中图分类号 O572.23

文献标志码 A

doi: 10.3788/LOP202259.0136001

1 Introduction

In quantum mechanics, the Hermiticity of physical observables guarantees the existence of real eigenvalues of a Hamiltonian. A recent remarkable discovery revealed that new infinite classes of parity-time (PT)-symmetry complex Hamiltonians, despite their non-Hermitian nature, can also have real eigenvalues. These PT-symmetric theories may be viewed as analytic continuations of conventional theories from real to complex spaces^[1-3].

Theoretical studies have been conducted on the dynamic evolution of quantum systems under the PT-symmetry Hamiltonian. It was proven that these Hamiltonians exhibit strange properties.

In many systems, the PT-symmetry Hamiltonian can be quantum simulated. The PT-symmetric non-Hermitian system has unconventional characteristics in classical optical systems^[4-13], microwave cavities^[14-16], quantum gases^[17], single nitrogen-vacancy centres in

diamonds^[18], and single photons^[19-21]. Xue *et al.* experimentally simulated non-unitary quantum dynamics using a single-photon interferometer network and studied the information flow between a symmetric non-Hermitian system and its environment^[22]. However, direct simulations of the PT-symmetry Hamiltonians and energy observation in a single-photon interferometer have not been studied. In this study, we experimentally simulated the PT-symmetric Hamiltonians directly instead of an effective Hamiltonian and obtained the energy eigenvalues of the simulated system from the experimental data for the first time. The PT phase transition is characterised by the observation of energy more intuitively and profoundly than other critical phenomena. Understanding the energy eigenvalues' change in the quantum regime provides a new and crucial perspective for studying open quantum systems and is useful for applications in quantum information.

收稿日期: 2021-11-04; 修回日期: 2021-11-08; 录用日期: 2021-11-11

通信作者: *anningzhang@bit.edu.cn

In this study, we used a single-photon interference network to simulate the quantum dynamics evolution in PT-symmetric non-Hermitian systems. We observed the exceptional point that the energy eigenvalues change from a PT-symmetry unbroken region to a PT-symmetry broken region. To study exceptional points, long-time quantum dynamics evolution is necessary. It is difficult to maintain long-time coherence and measure the long-time evolution in experiments. However, we overcame this difficulty by directly implementing non-unitary time-evolution operators at any given time and simulated the non-unitary quantum dynamics by performing non-unitary gate operations on the initial state. Then, for the quantum final state evolving over time, we used the quantum state tomography to obtain all information about the evolved quantum state. By inputting various initial states and measuring the final states, all information about non-unitary operators in the experiment could be obtained. The energy eigenvalues were extracted through an interferometric measurement^[23]. We obtained all information on the Hamiltonian in our quantum simulation using this method. Then, we obtained the energy eigenvalues of the simulated system.

To the best of our knowledge, this is the first time the process of the system from a PT-symmetric unbroken region to a PT-symmetry broken region using a single-photon interferometer and the corresponding energy eigenvalues change from real to imaginary with the Hamiltonian changing parameter are described.

2 Theory

The dynamic evolution of the system differed in the PT-symmetry unbroken and broken regions. The eigenvalues of the corresponding system were also different. Considering a two-level system, the parity operator is P , and the time reversal operator is T ^[1, 24-27].

$$\begin{cases} PxP = -x \text{ and } PpP = -p \\ TxT = x, TpT = -p, \text{ and } TiT = -i \end{cases} \quad (1)$$

where x and p are the position and momentum operators, respectively, and i is the imaginary unit. Canonical commutation relations such as $[x, p] = i\hbar$ are invariant under PT. In our experiment, the non-Hermitian Hamiltonian was given by

$$\mathbf{H}_{\text{PT}} = \begin{bmatrix} ia & 1 \\ 1 & -ia \end{bmatrix}, \quad (2)$$

where a is a real number. When $0 < a < 1$, the Hamiltonian was in a PT-symmetry unbroken region. The two eigenvalues of \mathbf{H} were $E_{\pm} = \pm\sqrt{1-a^2}$, and the eigenvalues were real. When $a > 1$, the system was in a PT-symmetry broken region, and the eigenvalues were imaginary.

For each given time t , there is $\mathbf{U} = \exp(-i\mathbf{H}_{\text{PT}}t)$, and \mathbf{H}_{PT} is given by Eq. 2. The non-unitary dynamic evolution of the system was captured by the final state density matrix:

$$\rho_{1,2}(t) = \frac{\exp(-i\mathbf{H}_{\text{PT}}t) \rho_{1,2}(0) \exp(i\mathbf{H}_{\text{PT}}^\dagger t)}{\text{Tr}[\exp(-i\mathbf{H}_{\text{PT}}t) \rho_{1,2}(0) \exp(i\mathbf{H}_{\text{PT}}^\dagger t)]}. \quad (3)$$

Initial density matrix $\rho_{1,2}(0) = |\mathbf{H}\rangle\langle\mathbf{H}|(|\mathbf{V}\rangle\langle\mathbf{V}|)$.

Considering $a=0.9$, $t=7.04$ as an example, the first, second, and third columns are the theoretical values of the final state density matrix passing through \mathbf{U} when the input states are $|\mathbf{H}\rangle$, $|\mathbf{V}\rangle$, and $(|\mathbf{H}\rangle - i|\mathbf{V}\rangle)/\sqrt{2}$. The first and second lines are the real and imaginary parts, respectively. So, we can calculate the experimental Hamiltonian from a known input state and the corresponding measured output state.

3 Experiment

Our experiment encoded the polarisation of a photon to $|\mathbf{H}\rangle = (1\ 0)^T$ and $|\mathbf{V}\rangle = (0\ 1)^T$. As shown in Fig. 1, the experimental setup comprised four modules designed for single-photon source preparation, initial state preparation, evolution, and final state measurement. We generated a heralded single-photon source using a method proposed in a previous study^[28]. A continuous-wave laser with a 405 nm wavelength and a 20 mW power was used as the pumping light source. After the pumped laser

passed through a periodically poled potassium titanyl phosphate crystal, orthogonal polarisation photon pairs with a central wavelength of 810 nm were created via spontaneous parametric down-conversion^[29-30]. One photon was used as a trigger, and another was used as a signal.

A single-photon source through a polarized beam splitter (PBS), a half wave plate (HWP), and a quarter wave plate (QWP) was prepared in the initial state $|H\rangle$ or $|V\rangle$, and then sent to a single photon interferometer such as Fig. 1.

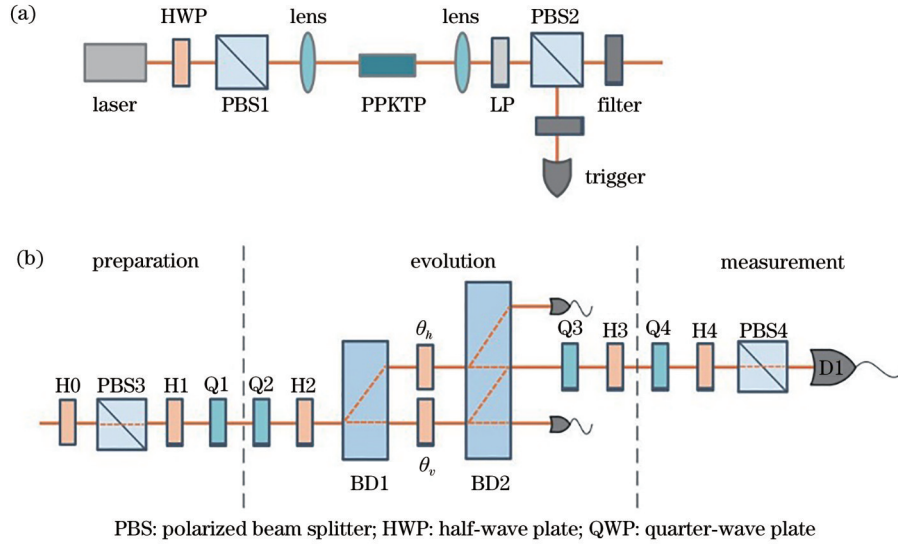


Fig. 1 Experimental setup. (a) Single-photon source preparation; (b) three parts are initial state preparation, evolution, and final state measurement from left to right in sequence

In the experiment, instead of realizing a non-Hermitian Hamiltonian, we directly implement a time evolution operator U with any given time, and obtain a final state of U acting on the initial state. As shown in Fig. 1, in the experiment U_{exp} was decomposed into

$$U_{\text{exp}} = R_2(\theta_2, \phi_2) L(\theta_h, \theta_v) R_1(\theta_1, \phi_1). \quad (4)$$

The rotation operator R_i is realized by a QWP of angle ϕ_i and an HWP of angle θ_i . A polarisation-dependent loss operator L was realized by combining two birefringent calcite beam displacers (BDs) and two HWPs with angles θ_h and θ_v . Here, six wave plate angles were determined by U .

The choice of the wave plate between two BDs is crucial. The offset of BD was 2.7 mm in our experiment, and the offset in Ref. [22] was 3 mm. Because 3 mm or 2.7 mm offset was small, and the commonly used framework of the wave plate is too big to be inserted only in the upper or lower path, wave plates in Ref. [22] were used without stents. Different wave plate angles adjusted for all data points in the experiment caused considerable

difficulty and experimental error. We further studied the theory and found that there were multiple combinations of θ_h and θ_v that could obtain the same evolution operator. Therefore, we designed an algorithm to search multiple groups of angles that satisfied the theory and selected the same angle of θ_h and θ_v from them to perform experiments, which reduced the difficulty of the experiment. Considering $a=0.3$ as an example, we could set θ_h and θ_v to be 22.5° in this case. When θ_h and θ_v were equal, the HWP across the two paths was allowed to be used in the experiment. The algorithm clearly showed the evolution operator and wave plate angle as well as revealed the corresponding relationship between experiment and theory, which is helpful in the experimental design of the non-Hermitian PT-symmetric Hamiltonian.

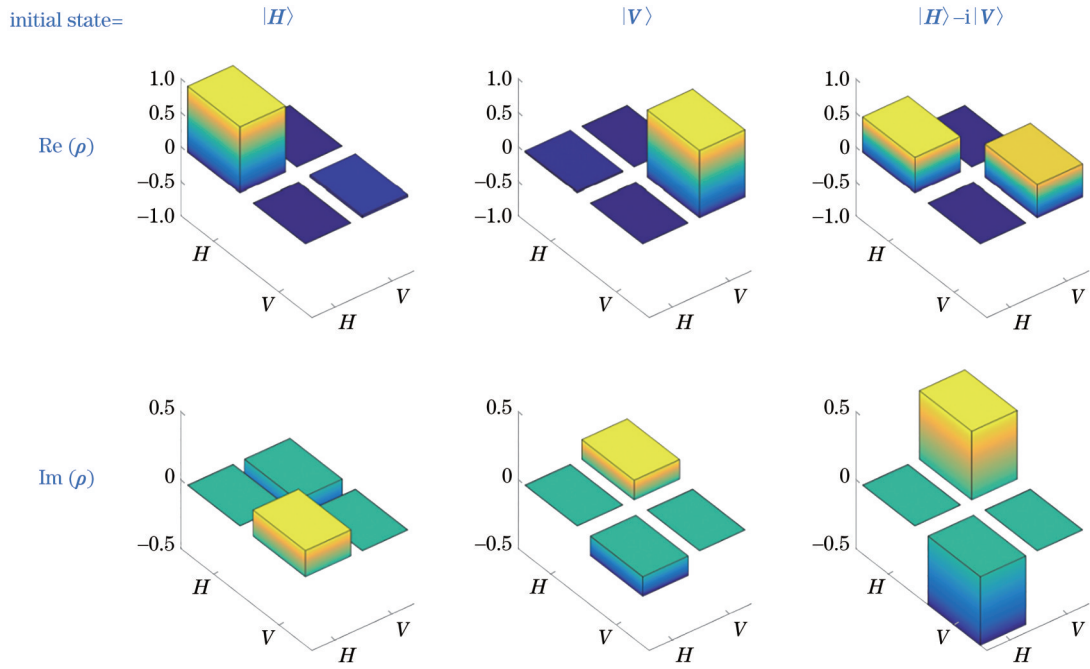
If two paths pass through the same wave plate, a commercial wave plate can be used in the experiment. The algorithm had the advantages of high adjustable precision, and the upper and lower experimental errors cancelled each other, which

reduced the difficulty and improved the accuracy of the experiment.

After signal photons passed through the interferometric setup, the final state density matrix, represented by \mathbf{U}_{exp} , was

$$\rho_{1,2}(t) = \frac{\mathbf{U}_{\text{exp}} \rho_{1,2}(0) \mathbf{H}_{\text{exp}}^\dagger}{\text{Tr}[\mathbf{U}_{\text{exp}} \rho_{1,2}(0) \mathbf{H}_{\text{exp}}^\dagger]}. \quad (5)$$

Initial density matrix $\rho_{1,2}(0) = |\mathbf{H}\rangle\langle\mathbf{H}|(|\mathbf{V}\rangle\langle\mathbf{V}|)$. Using the quantum state tomography technology, we could reconstruct the final state density matrix. The theoretical and experimental values of the final state density matrix



By inputting different initial states, such as $|\mathbf{H}\rangle$ and $|\mathbf{V}\rangle$, we reconstructed the time-evolution matrix \mathbf{U}_{exp} according to Eq. 5. \mathbf{H}_{exp} could be obtained from \mathbf{U}_{exp} using $\mathbf{U} = \exp(-i\mathbf{H}_{\text{PT}}t)$. a_{exp} could be obtained from \mathbf{H}_{exp} using Eq. 2. The energy eigenvalues of the experimental system could be obtained by substituting $E_{\text{exp}\pm} = \pm\sqrt{1 - a_{\text{exp}}^2}$. The eigenvalues obtained from this method are shown in Figs. 4 and 5.

$a > 0$ guaranteed non-Hermitian, and when $a = 0$, Hamiltonian became Hermitian. When $0 < a < 1$, the system was in the PT-symmetry unbroken region. As shown in Figs. 4 and 5,

are shown in Fig. 2 and Fig. 3, respectively. Measurement was implemented with a combination of HWP, QWP, and PBS. In fact, in this experiment, owing to the particularity of the simulated Hamiltonian, only two initial input states \mathbf{H} and \mathbf{V} were necessary, and the measurement of their \mathbf{H} and \mathbf{V} bases could fully describe the process. We measured the probabilities of photons in the only two bases $\{|\mathbf{H}\rangle, |\mathbf{V}\rangle\}$. In this process, all photon countings were consistent with the trigger photon. The experimental coincidence count was about 2500 counts per second.

eigenvalue E_+ remained real and gradually decreased as a approached 1 from 0. When $a > 1$, the system was in the PT-symmetry broken region. The real part of eigenvalue E_+ equalled zero and the imaginary part appeared as a approached 1.5 from 1. The exceptional point was located at $a = 1$. E_- is the opposite of E_+ , so their change rules were similar.

4 Conclusion

The phase transition can be described by the eigenvalues of the PT-symmetric Hamiltonian from experimental data [18]. In this study, we used a single-photon interference network to simulate the symmetric non-unitary quantum dynamics evolution.

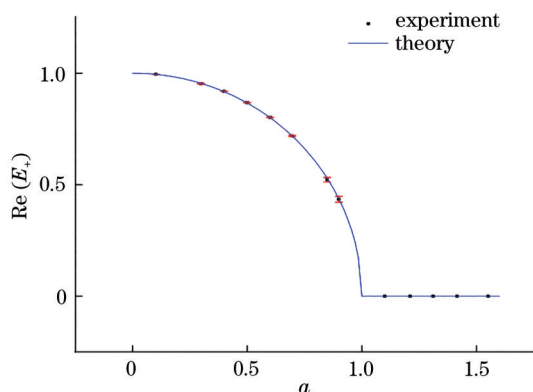
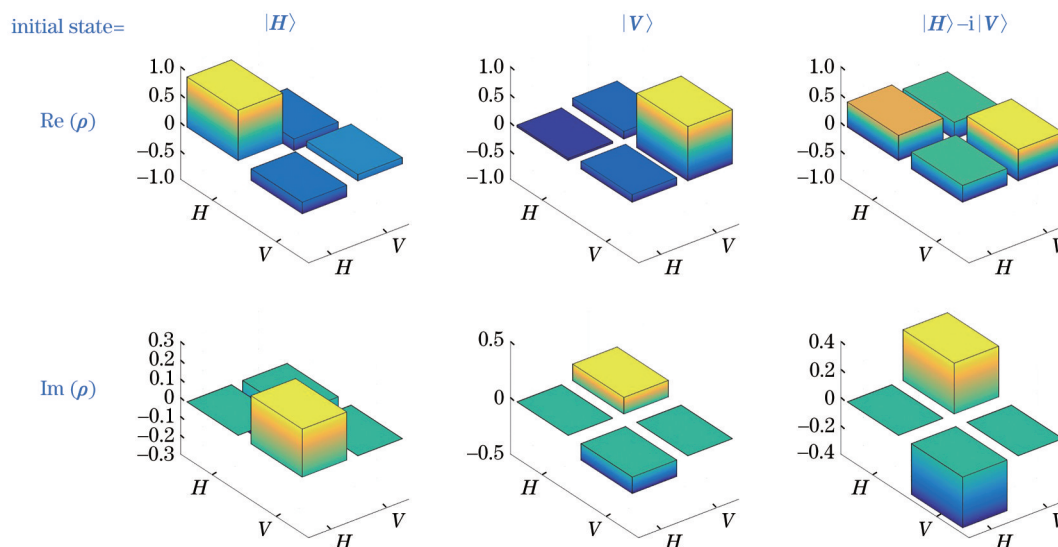


Fig. 4 Experimental observation of the breaking of the PT-symmetry (real part of eigenvalue E_+ decreases when $0 < a < 1$ and equals zero when $a > 1$)

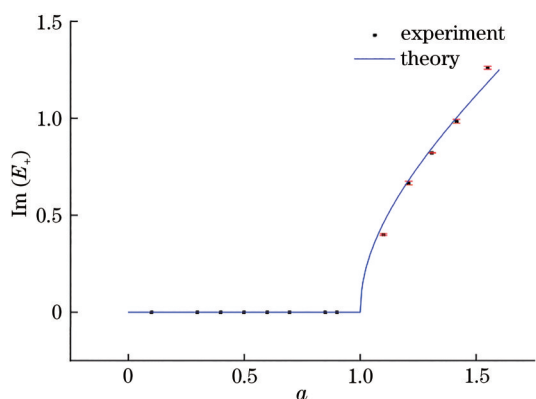


Fig. 5 Experimental observation of the breaking of the PT-symmetry (imaginary part of eigenvalue E_+ equals zero when $0 < a < 1$ and increases when $a > 1$)

We directly built the time-evolution matrix U for any given time using a combination of optical elements. Then, the final state density matrix was obtained by quantum state tomography.

The time-evolution matrix U was reconstructed by inputting different initial states. The PT-symmetric Hamiltonian was obtained from experimental data. Finally, the eigenvalue of the PT-symmetric Hamiltonian in the experiment was obtained, which intuitively showed the phenomenon that the energy changes from real to imaginary during the system maintenance from PT-symmetry unbroken region to PT-symmetry broken region. The experimental results showed excellent agreement with the corresponding theoretical predictions and proved the correctness of PT-symmetry theory.

We intuitively showed the exceptional points of PT-symmetric non-unitary quantum dynamics in a single-photon interference network from the energy perspective. We also proved that a linear optical system with single-photon source could simulate the non-Hermitian system, which could be used to study the physical problems in non-Hermitian systems, such as new topological invariants^[31-34], quantum thermodynamics^[27] and information criticality^[35]. Our experimental system provides a platform for studying open systems with dissipation and loss.

Acknowledgements

This work is supported by National Key R & D Program of China (2018YFB0504303).

References

- [1] Bender C M, Boettcher S. Real spectra in non-Hermitian Hamiltonians having PT symmetry[J]. *Physical Review Letters*, 1998, 80(24): 5243-5246.
- [2] Heiss W D. The physics of exceptional points[J]. *Journal of Physics A: Mathematical and Theoretical*, 2012, 45(44): 444016.
- [3] El-Ganainy R, Makris K G, Khajavikhan M, et al. Non-Hermitian physics and PT symmetry[J]. *Nature Physics*, 2018, 14(1): 11-19.
- [4] Guo A, Salamo G J, Duchesne D, et al. Observation of PT-symmetry breaking in complex optical potentials [J]. *Physical Review Letters*, 2009, 103(9): 093902.
- [5] Rüter C E, Makris K G, El-Ganainy R, et al. Observation of parity-time symmetry in optics[J]. *Nature Physics*, 2010, 6(3): 192-195.
- [6] Chong Y D, Ge L, Stone A D. PT-symmetry breaking and laser-absorber modes in optical scattering systems[J]. *Physical Review Letters*, 2011, 106(9): 093902.
- [7] Regensburger A, Bersch C, Miri M A, et al. Parity-time synthetic photonic lattices[J]. *Nature*, 2012, 488(7410): 167-171.
- [8] Liertzer M, Ge L, Cerjan A, et al. Pump-induced exceptional points in lasers[J]. *Physical Review Letters*, 2012, 108(17): 173901.
- [9] Brandstetter M, Liertzer M, Deutsch C, et al. Reversing the pump dependence of a laser at an exceptional point[J]. *Nature Communications*, 2014, 5: 4034.
- [10] Weimann S, Kremer M, Plotnik Y, et al. Topologically protected bound states in photonic parity-time-symmetric crystals[J]. *Nature Materials*, 2017, 16(4): 433-438.
- [11] Hodaei H, Hassan A U, Wittek S, et al. Enhanced sensitivity at higher-order exceptional points[J]. *Nature*, 2017, 548(7666): 187-191.
- [12] Wimmer M, Miri M A, Christodoulides D, et al. Observation of Bloch oscillations in complex PT-symmetric photonic lattices[J]. *Scientific Reports*, 2015, 5: 17760.
- [13] Feng L, Xu Y L, Fegadolli W S, et al. Experimental demonstration of a unidirectional reflectionless parity-time metamaterial at optical frequencies[J]. *Nature Materials*, 2013, 12(2): 108-113.
- [14] Peng B, Özdemir Ş K, Lei F C, et al. Parity-time-symmetric whispering-gallery microcavities[J]. *Nature Physics*, 2014, 10(5): 394-398.
- [15] Poli C, Bellec M, Kuhl U, et al. Selective enhancement of topologically induced interface states in a dielectric resonator chain[J]. *Nature Communications*, 2015, 6(1): 1-5.
- [16] Liu Z P, Zhang J, Özdemir Ş K, et al. Metrology with PT-symmetric cavities: enhanced sensitivity near the PT-phase transition[J]. *Physical Review Letters*, 2016, 117(11): 110802.
- [17] Li J M, Harter A K, Liu J, et al. Observation of parity-time symmetry breaking transitions in a dissipative Floquet system of ultracold atoms[J]. *Nature Communications*, 2019, 10: 855.
- [18] Wu Y, Liu W Q, Geng J P, et al. Observation of parity-time symmetry breaking in a single-spin system [J]. *Science*, 2019, 364(6443): 878-880.
- [19] Tang J S, Wang Y T, Yu S, et al. Experimental investigation of the no-signalling principle in parity-time symmetric theory using an open quantum system [J]. *Nature Photonics*, 2016, 10(10): 642-646.
- [20] Xiao L, Zhan X, Bian Z H, et al. Observation of topological edge states in parity-time-symmetric quantum walks[J]. *Nature Physics*, 2017, 13(11): 1117-1123.
- [21] Wang K K, Qiu X Z, Xiao L, et al. Observation of emergent momentum-time skyrmions in parity-time-symmetric non-unitary quench dynamics[J]. *Nature Communications*, 2019, 10(1): 1-8.
- [22] Xiao L, Wang K K, Zhan X, et al. Observation of critical phenomena in parity-time-symmetric quantum dynamics[J]. *Physical Review Letters*, 2019, 123(23): 230401.
- [23] Wang K K, Xiao L, Budich J C, et al. Simulating exceptional non-Hermitian metals with single-photon interferometry[J]. *Physical Review Letters*, 2021, 127(2): 026404.
- [24] Bender C M, Brody D C, Jones H F. Must a Hamiltonian be Hermitian? [J]. *American Journal of Physics*, 2003, 71(11): 1095-1102.
- [25] Bender C M, Brody D C, Jones H F. Complex extension of quantum mechanics[J]. *Physical Review Letters*, 2002, 89(27): 270401.
- [26] Bender C M. Making sense of non-Hermitian Hamiltonians[J]. *Reports on Progress in Physics*, 2007, 70(6): 947-1018.
- [27] Deffner S, Saxena A. Jarzynski equality in PT-symmetric quantum mechanics[J]. *Physical Review Letters*, 2015, 114(15): 150601.

- [28] Hong C K, Mandel L. Experimental realization of a localized one-photon state[J]. *Physical Review Letters*, 1986, 56(1): 58-60.
- [29] Chen X X, Yang J Z, Chai X D, et al. Single-photon Bell state measurement based on a quantum random walk[J]. *Physical Review A*, 2019, 100(4): 042302.
- [30] Yang J Z, Li M F, Chen X X, et al. Single-photon quantum imaging via single-photon illumination[J]. *Applied Physics Letters*, 2020, 117(21): 214001.
- [31] Dembowski C, Gräf H D, Harney H L, et al. Experimental observation of the topological structure of exceptional points[J]. *Physical Review Letters*, 2001, 86(5): 787-790.
- [32] Yao S Y, Song F, Wang Z. Non-Hermitian Chern bands[J]. *Physical Review Letters*, 2018, 121(13): 136802.
- [33] Gong J B, Wang Q H. Geometric phase in PT-symmetric quantum mechanics[J]. *Physical Review A*, 2010, 82: 012103.
- [34] Ghatak A, Das T. New topological invariants in non-Hermitian systems[J]. *Journal of Physics: Condensed Matter*, 2019, 31(26): 263001.
- [35] Kawabata K, Ashida Y, Ueda M. Information retrieval and criticality in parity-time-symmetric systems[J]. *Physical Review Letters*, 2017, 119(19): 190401.